

Part I: Computing and Numerical Methods

Report:

Case Study of Numerical Schemes for Solving second-order ODEs

Q1(a)

$$\frac{d^2y}{dt^2} + \omega^2 y(t) = 0 \quad (1)$$

The Analytical solution to the equation above (1) can be found by considering harmonic functions as solutions, using the complex exponential:

$$y(t) = Ae^{(\omega t)i} \quad (2)$$

$$\frac{d^2y}{dt^2} = -A\omega^2 e^{(\omega t)i} \quad (3)$$

Evaluating our equation by substituting our complex exponential,

$$-A\omega^2 e^{(\omega t)i} + A\omega^2 e^{(\omega t)i} = 0 \quad (4)$$

So, our complex exponential satisfies the second-order ODE. Rewriting using Euler's identity:

$$\begin{aligned} y(t) &= Ae^{(\omega t)i} = B\cos(\omega t + \varphi) \\ &= B\cos\left(\sqrt{\frac{\rho_t g}{\rho L}} t + \varphi\right) \end{aligned} \quad (5)$$

Q1(b)

We arrive at the constants for our model:

$$\omega^2 = 19.62 \text{ rad}^2/\text{s}^2, \quad B = 0 \text{ m}$$

Hence giving the equation and graph below for the interval. $t: [0,10]$,

$$y(t) = 0.1\cos(4.4294t) \quad (7)$$

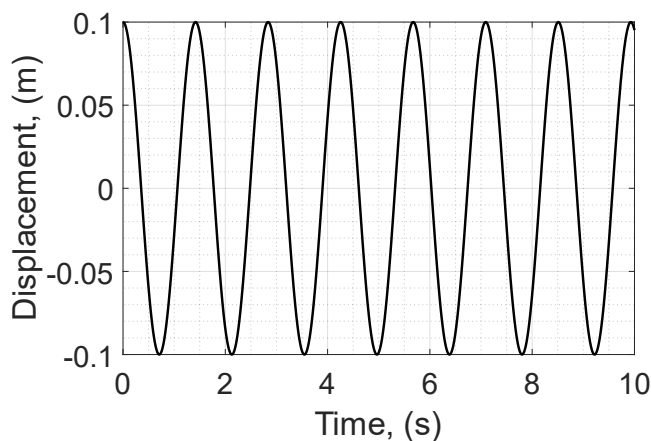


Figure 1: Analytical Solution

$$\dot{\mathbf{Y}} = \mathbf{A}\mathbf{Y} \quad (8)$$

$$\begin{bmatrix} \dot{y} \\ \dot{\dot{y}} \end{bmatrix} = \begin{bmatrix} 0 & 1 \\ -\omega^2 & 0 \end{bmatrix} \begin{bmatrix} y \\ \dot{y} \end{bmatrix} \quad (9)$$

$$\text{Q1(d)} \quad \text{Eigenvalues: } \lambda_{1/2} = \pm 4.4294i$$

The Eigenvalues indicate the Numerical Stability of the system. Since the Eigenvalues are Purely Imaginary the system is unstable for all time steps. Therefore, there is no maximum time step for FE which will never converge. But the maximum convergent timesteps for RK4 lies around $\sim 0.64\text{m}$ and the theoretical max time step is 0.6389m .

For RK4 stability: [1]

$$\text{Im}(h_{\max}\lambda) = 2.83$$

$$h_{\max} = \frac{2.83}{4.4294} = 0.6389$$

Q2(a)

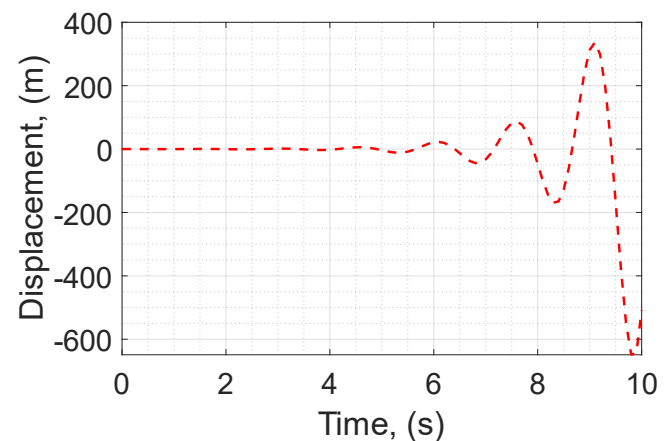


Figure 2: Explicit Euler Scheme

Q2(b)

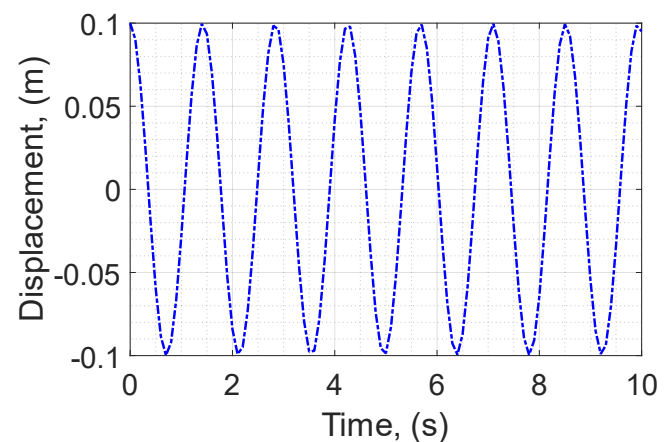


Figure 3: Runge-Kutta, 4th Order Scheme

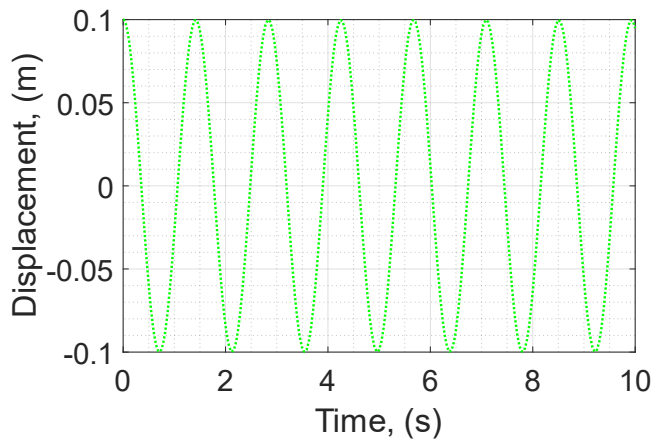
Q2(c)

Figure 4: MATLAB™ ode45 in-built function.

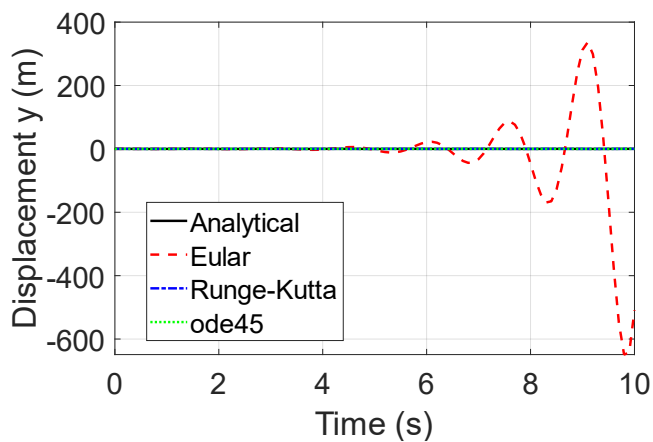
Q2(d)

Figure 5: Comparison of Solutions

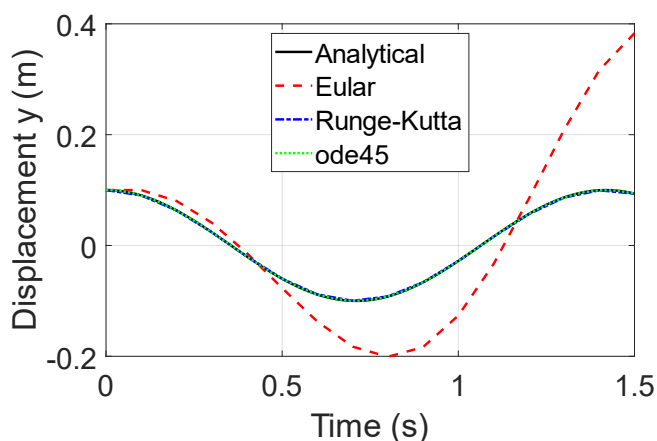


Figure 6: Comparison of Solutions Zoomed

Figure 5 shows that RK4 and ode45 produce stable solutions with low error relative to the analytical solution. However, the FE, which diverges rapidly, is an unstable solution for this time step and range. Figure 6 shows the period of oscillation increases over time for FE whilst ode45 and RK4 follow the analytical solution closely.

Overall, the FE is a bad approximation of the system compared to RK4 and ode45.

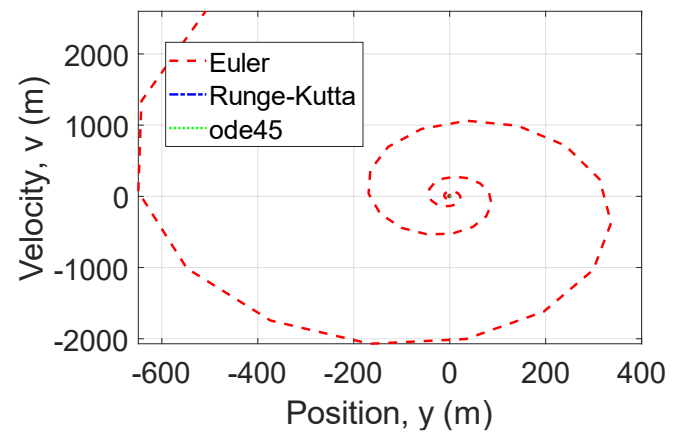
Q2(e)

Figure 7: Velocity vs Displacement for all Schemes.

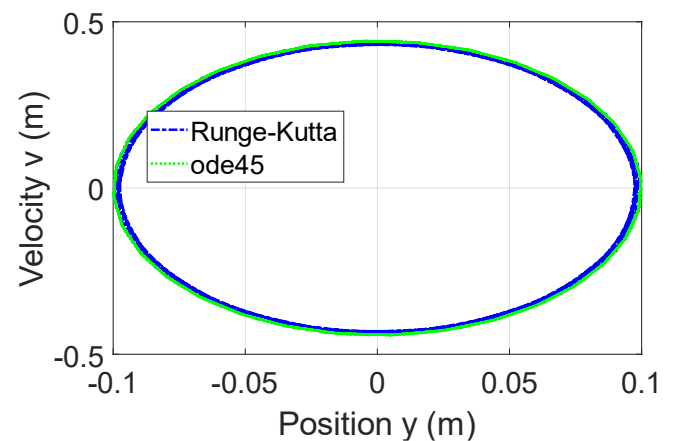


Figure 8: Velocity vs Displacement for Bounded Stable Schemes

Figure 7 shows the velocity vs time response of the FE is very unstable indicating a diverging spiral showing the FE is a poor model of the system and it has a high error propagation causing this response. The RK4 and ode45 solutions cannot be seen clearly in Figure 7. For Figure 8, the Velocity and Displacement response can be seen clearly with the RK4 and ode45 remaining bounded by an oval close to the analytical solution. Showing their stable characteristics

Q2(f)(i)

The reliability of the solutions can be measured by their numerical stability. The FE is highly unstable for all time steps due to the inherent numerical instability of the system due to purely imaginary Eigenvalues. This can be seen in the highly divergent displacement vs time response

shown by FE in Figures 2,5 and 6 which is out of line with the analytical solution.

Additionally, the Velocity vs displacement plots shown in Figures 7 and 8 depict the highly unrealistic physical response of the system with increasing Velocities and displacements.

The RK4 and ode45 solutions depict numerically stable solutions in Figures 3,4,5 and 6. The RK4 and ode45 solutions follow closely to the analytical solution with similar displacements and periods of oscillation. So are good representations of the physical system.

Q2(f)(ii)

In terms of Computational Complexity, the RK4 is more computationally expensive for each timestep compared to the FE but larger step sizes can be used compared to FE, whilst still obtaining sufficiently accurate results. Thus, the increased accuracy of RK4 makes up for the increase in required computational power.

Q3(a)

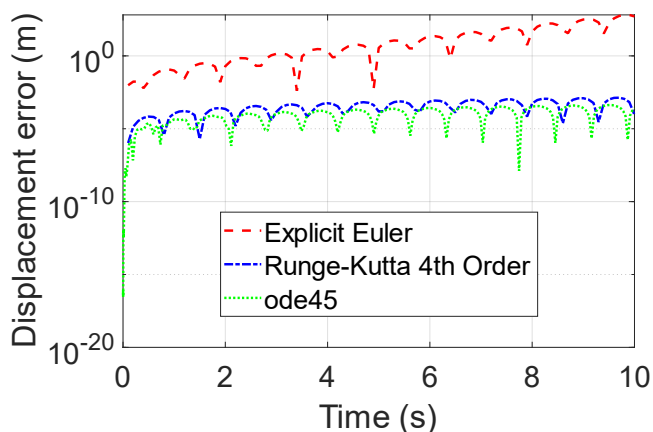


Figure 9: Absolute Relative Error Plot to Analytical Solution

With all the methods the relative error is similar for ode45 and RK4 but is about five orders of magnitude higher for FE. This is due to the inherent instability of FE as it grows rapidly uncoordinated with the analytical solution. RK4 and ode45 remain stable and bounded with errors increasing over time. This increase in error is characteristic of any numerical scheme. Hence the most accurate results are from the RK4 and ode45 due to the lower average error.

Q3(b)

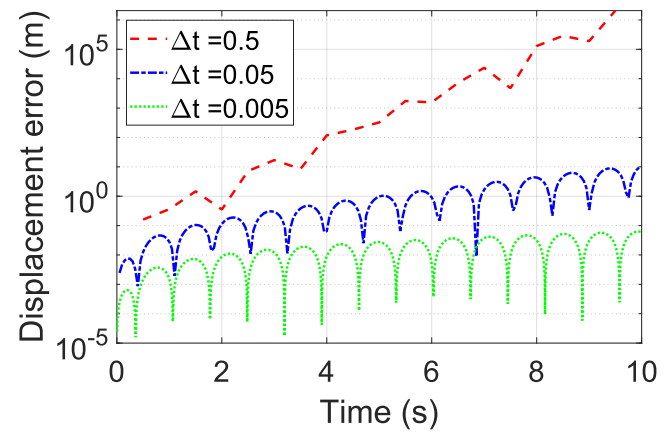


Figure 10: Absolute Relative Error Plot to Analytical Solution, FE

For all the time steps the FE is unstable with the errors increasing over time with the larger time steps showing the largest errors. And the smaller time steps have the highest relative accuracy. The high increase over time can be attributed to the unstable nature of the system which produces an unstable FE solution.

Q3(c)

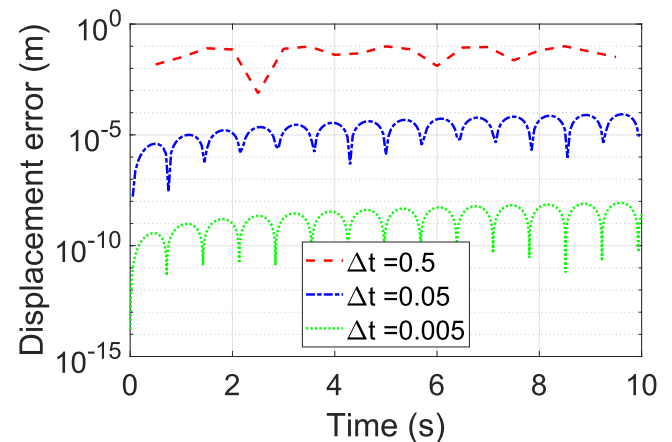


Figure 11: Absolute Relative Error Plot to Analytical Solution, RK4

For all the time steps the RK4 is stable with the errors increasing over time with larger time steps showing the largest errors. And the smaller time steps with the highest relative accuracy. The low increase in error over time can be attributed to the stable nature of the system which produces a stable RK4 solution.

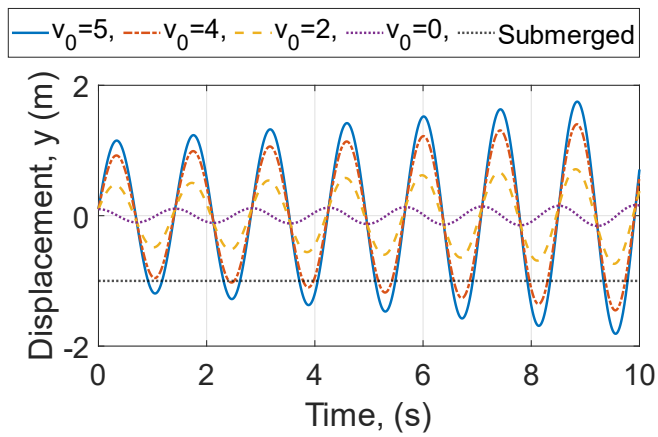
Q3(d)

Figure 12: Varying Initial Conditions, FE

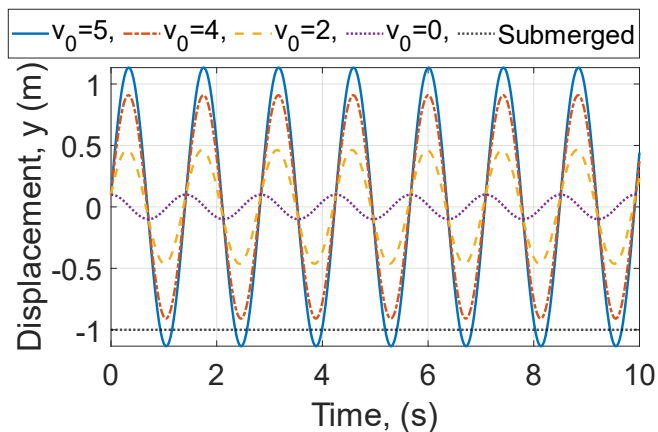


Figure 13: Varying Initial Conditions, RK4

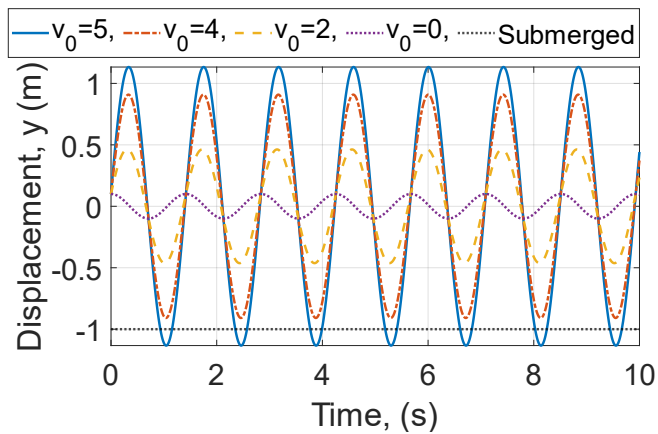


Figure 14: Varying Initial Conditions, Analytical Solution

Varying the initial velocity in Figures 12, 13, and 14 as velocity increases the amplitude of oscillations increases however the period of oscillations remains constant. The vessel is fully submerged between initial velocities. 4 m/s and 5 m/s. The vessel becomes submerged but never sinks into the water no matter the initial velocity.

Q4(a) Compared to the mass-spring model the buoyancy model acts in the vertical direction with gravitational effects which have not been included in the modelled equation. The spring-mass system does not include these effects.

The mathematical formulation of the system is equivalent as both models have a restoring force promoting oscillations with resistive forces causing damping.

Difficulties arose when making the comparison of the Explicit Euler and the other schemes due to the instability of the system, we were using.

Q4(b) Including Damping, with c Being our damping coefficient changes our equation of motion to:

$$\frac{d^2y}{dt^2} + c \frac{dy}{dt} + \omega^2 y(t) = 0 \quad (10)$$

$$\begin{bmatrix} \dot{y} \\ \ddot{y} \end{bmatrix} = \begin{bmatrix} 0 & 1 \\ -\omega^2 & -c \end{bmatrix} \begin{bmatrix} y \\ \dot{y} \end{bmatrix} \quad (11)$$

Q4(b)(i) The damped system has an increasing period and decreasing amplitude over time. However, the undamped case shows a constant period and amplitude.

Q4(b)(ii) The effects of damping on numerical stability include increasing the stability of solutions due to the inclusion of a dissipative mechanism that prevents runaway solutions. Additionally, it ensures solutions remain bounded as energy is dissipated over time and the scheme is unlikely to diverge.

Q4(b)(iii) $y(t) = 0.1e^{-0.1t}\cos(4.4283t) \quad (12)$

Q4(b)(iv)

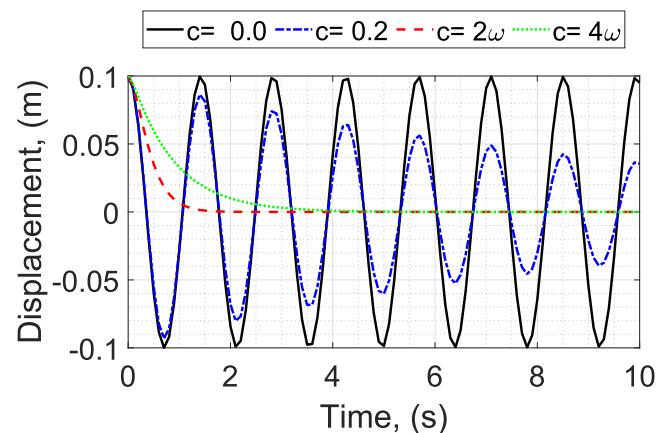


Figure 15: Damped Solution, RK4. $c = 0$ (undamped), $c = 0.2$ (underdamped), $c = 2\omega$ (critical damped), $c = 4\omega$ (overdamped)

References:

[1] (Figure 4.8) Moin P. Fundamentals of Engineering Numerical Analysis. 2nd ed. Cambridge University Press; 2010.